AI and the magnetic tensor for quick depth estimation

D. Pratt[1], K. McKenzie[1], A. White[1]
1. Tensor Research, Australia,
David.Pratt@tensor-research.com.au

BIOGRAPHY

David Pratt is a director of Tensor Research. He holds a B.Sc. (Hons) and M.Sc. from the University of Sydney in Geology and Geophysics and a Ph.D. in Physics, University of Newcastle. His early career included the NSW Geological Survey, seismic processing company Digitech and Layton Geophysical Consultants. In 1979 he worked as a geophysical consultant and in 1984 he co-founded Encom Technology. He was Managing Director from 2001 until it was acquired by Pitney Bowes Business Insight in 2007. In 2010 he started Tensor Research with two colleagues to focus on advanced potential fields research. He received the ASEG's Grahame Sands Award in 2010.

SUMMARY

Eigenvector analysis of the magnetic gradient tensor is combined with an artificial intelligence (AI) approach to rapid, interactive estimation of depth to magnetic source for a variety of geological target shapes. The method uses the flight line data for maximum depth resolution and grids of the magnetic gradient tensor and other parameters for 2D spatial attributes. The magnetic gradient tensor and related parameters are computed using FFT processing of the original total magnetic intensity grid. The eigenvectors are used to compute the normalised source strength (NSS), dimensionality, azimuth, centre of magnetisation and susceptibility. If the target is pipe-like or an ellipsoid in shape, then the eigenvector is used to compute the dip of the magnetisation vector. This information is then used to constrain some classic depth interpretation techniques that include the tensor, Euler 2D, Euler 3D, Peters Length, Werner Deconvolution and Tilt methods.

Key words: magnetic, tensor, depth, AI, magnetisation

INTRODUCTION

Wikipedia defines AI as "artificial intelligence, the intelligence of machines and robots" while Thesaurus.com suggests expert systems, machine learning and neural networks. Our expert system approach was inspired by an early project that automatically built 3D seed models for inversion (Pratt et al., 2001). The AI expert system is designed as a productivity tool to speed up the process of interactive magnetic depth interpretation without the need to perform a geophysical inversion. We have combined the inherent high precision of the original line data with the spatial information that is present in the gridded total magnetic intensity (TMI) data to extract parameters that are well suited for input to an AI expert system. These parameters make it possible to locate the anomaly, detect the geological model style and estimate the target orientation, depth and magnetic properties. This is a very simple expert system that is designed to speed up the process of depth interpretation.

The magnetic tensor provides the foundation for much of the decision making that takes place in the AI system. It is computed from the TMI grid using FFT transformation along with other parameters such as the magnetic field components, gradients, tilt and reduction to pole (RTP) (Pratt et al., 2018). These two-dimensional (2D) parameters are then resampled onto the original flight lines to form the primary dataset for the AI system (Figure 1).

Once the AI system has located the anomaly and suggested a model style, it computes the depth, azimuth and magnetic properties for the target using a range of conventional depth interpretation methods including the tensor, Euler 2D, Euler 3D, Werner Deconvolution, Peters Length and Tilt Depth. The depth methods support different model styles, but together provide a useful range of model shapes that include dykes, formations, pipes, channels, plutons and boundaries. Importantly, the suggested model style can be overridden by the interpreter. The variability between methods provides guidance on uncertainty and also educates the user on the impact of geological style (constraint) on the precision of the depth estimation.

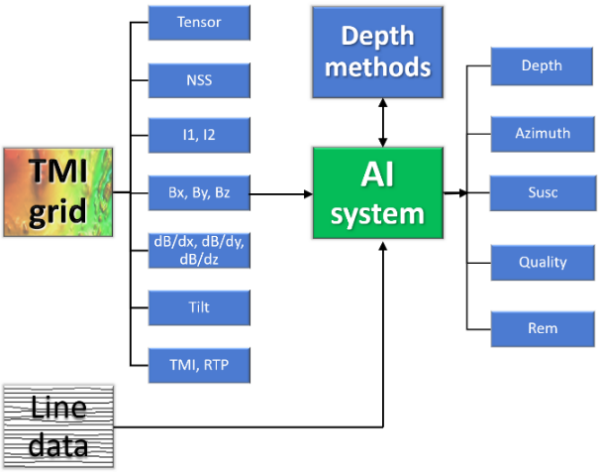


Figure 1. Schematic concept of the processes associated with the AI processing where the primary data is converted to processed channels that are required for input to the depth methods and soft AI processes. The grid data provide the essential 2D information while the line data provide the best precision for depth estimation.

The AI system also determines the level of interference between overlapping anomalies and provides the user with feedback on the quality of the depth estimate.

IMPORTANT TENSOR PROPERTIES

The magnetic tensor has many characteristics that provide important parametric information for the AI system. It is defined in equation 1,

$$\Gamma = \begin{bmatrix} B_{xx} & B_{xy} & B_{xz} \\ B_{yx} & B_{yy} & B_{yz} \\ B_{zx} & B_{zy} & B_{zz} \end{bmatrix} = \begin{bmatrix} \frac{\partial B_x}{\partial x} & \frac{\partial B_x}{\partial y} & \frac{\partial B_x}{\partial z} \\ \frac{\partial B_y}{\partial x} & \frac{\partial B_y}{\partial y} & \frac{\partial B_y}{\partial z} \\ \frac{\partial B_z}{\partial x} & \frac{\partial B_z}{\partial y} & \frac{\partial B_z}{\partial z} \end{bmatrix} \quad (1)$$

where $B_{ij} = \partial B_i / \partial j$ (for $i, j = x, y, z$) is the gradient of the i^{th} magnetic field component in the j^{th} axis direction.

Eigenvector decomposition of the symmetric tensor matrix produces a rotated and simplified version of the tensor (Λ) (Pedersen & Rasmussen, 1990, Clark 2012).

$$\underline{\mathbf{\Lambda}} = \begin{bmatrix} \lambda_1 & 0 & 0 \\ 0 & \lambda_2 & 0 \\ 0 & 0 & \lambda_3 \end{bmatrix} \quad (2)$$

where $\lambda_1 > \lambda_2 > \lambda_3$ are the eigenvalues of the magnetic gradient tensor (Pedersen and Rasmussen, 1990; Clark, 2012). They derive several parameters from the eigenvalues that are important for extracting useful geological characteristics from the target anomalies.

The rotational invariants I1 and I2 are defined as:

$$I_1 = B_{xx}\, B_{yy} + B_{yy}\, B_{zz} + B_{xx} - B_{xy}^2 - B_{yz}^2 - B_{xz}^2 \quad (3)$$

$$I_2 = B_{xx}\,(B_{yy}B_{zz} - B_{yz}^2) + B_{xy}\,(B_{yz}B_{xz} - B_{xy}B_{zz}) + B_{xz}\,(B_{xy}B_{yz} - B_{xz}B_{yy}) \quad (4)$$

The dimensionality index is defined as:

$$I = -\left(\frac{(I_2/2)^2}{(I_1/3)^3}\right) \quad (5)$$

This parameter is very important because it can tell us if the target is pipe-like (~1) or has extended strike (~0). It provides the AI system with a numeric value that can separate pipes from dykes and a continuum in between. A pluton with an elliptic shape could have a D_i value of around 0.5 to 0.75. This one parameter helps provide important information that feeds into depth and magnetic susceptibility estimation. The dimensionality index does vary with magnetisation direction and is more reliable at higher field inclinations.

If the dimensionality is low, then the source also has a strike or azimuth direction that can be computed from the tensor components (Pedersen & Rasmussen, 1990).

$$\tan(2\,\theta_s) = 2\frac{\left[B_{xy}\left(B_{xx} + B_{yy}\right) + B_{xz}B_{yz}\right]}{(B_{xx}^2 - B_{zz}^2 + B_{xz}^2 - B_{yz}^2)} \quad (6)$$

where, θ_s is the strike direction of the longer axis of the magnetic source.

Parameters derived from NSS

We only need to calculate the dimensionality index and strike direction at the centre of magnetisation rather than as continuous functions. Clark (2012) further developed the concept of normalised source strength (NSS, μ) (originally developed by Wilson, 1985) as an important parameter that could be derived from the magnetic gradient tensor.

$$\mu = \sqrt{(-\lambda_2^2 - \lambda_1\lambda_3)} \text{ where } \lambda_1 > \lambda_2 > \lambda_3 \quad (7)$$

It has many special characteristics because it is semi-independent of the source magnetisation direction. The NSS parameter peaks over the centre of magnetisation for discrete bodies and along the central axis of elongate sources. For wide sources, NSS peaks over the edge and for narrower targets, the maximum gradient locations of the NSS anomaly profile define the outer limits of the high magnetisation zone. If the depth-to-width ratio is less than 1, then we cannot resolve the true location of the edge, but we can define its maximum possible lateral extent or a susceptibility - thickness product.

We use Nelson's formulation (Nelson, 1988) to compute an estimate for the apparent magnetic susceptibility.

$$k = 0.625\, z\, T_{g0} / (B_{IGRF}(\sin^2 I_f + \cos^2 D_f)) \quad (8)$$

where the total gradient is defined as;

$$T_{g0} = \sqrt{(B_{xx}^2 + B_{yy}^2 + B_{zz}^2)} \quad (9)$$

and
z = target depth below the sensor,
B_{IGRF} = inducing field strength,
I_f = field inclination,
D_f = field declination.

A first order detection for remanence is determined by a sign reversal of the vertical gradient component B_{zz} or the first invariant I_1 at the centre of magnetisation.

Beike et al (2012), Clark (2014) and McKenzie (2019) show that the inclination ϕ of the magnetisation of a compact source (including a dipole, sphere, ellipsoid and vertical pipe) can be calculated from the tensor measurement over the centre of magnetisation using the following formula:

$$\phi = \cos^{-1}(\lambda_2/\mu) - \frac{\pi}{2} \quad (0 \leq \phi \leq \pi) \quad (10)$$

where λ_2 is the second eigenvalue and μ is the normalised source strength.

DEPTH INTERPRETATION METHOD

From the magnetic tensor over the centre of magnetisation and the NSS profile, we recover many geological attributes for each target anomaly;

- Target style - pipe, elliptic pluton or dyke-like,
- Strike direction for elongate targets,
- Centre of magnetisation (origin),
- Apparent magnetic susceptibility,
- Magnetic reversals,
- Magnetisation inclination, declination,
- Target edges.

This information is used to constrain and improve the precision of the depth determination. The geophysical methods we use include;

- Tensor,
- Euler 2D,
- Peters Length,
- Werner Deconvolution,
- Tilt Depth,
- Euler 3D.

We use the peak of the normalised source strength (NSS) from Clark (2014) to define the horizontal location of the centre of magnetisation which simplifies the calculations of depth for the Euler 2D, Werner and Tilt Depth methods. Depths are computed using a gradient analysis method proposed by Peters (1929), but modified for the NSScurve. The strike direction of the anomaly (Pedersen and Rasmussen, 1990) is used to correct the depth estimates for acute angled flight lines for the Tensor, Peters Length, Werner Deconvolution and Tilt Depth methods.

The tensor analysis provides a dimensionality index (Equation 5) which automatically differentiates between pipe-like magnetic sources and linear magnetic formations or dykes. This allows for different depth correction techniques to be applied according to the geology. Some methods such as Euler 2D analysis are very sensitive to an incorrect choice of the geological magnetic source type. Analysis of the NSS profile provides some information about the width of the magnetic source and the AI system classifies it as thin, intermediate or thick according to the body type selection.

Euler 2D Method
The Euler method is based on the original work by Thompson (1982) which is simplified as follows by using the normalised source strength derived centre of magnetisation,

$$z_0 = \frac{n\, B_{res}}{\partial B_m / \partial z} \qquad (11)$$

where;
B_m is the total magnetic field intensity at the centre of magnetisation,
B_{res} is the residual total field anomaly,
z_0 is the depth,
n is the structural index.

The structural index is normally defined in terms of poles and dipoles, but these terms have a physical geological equivalence as follows;

n = 1 is a line of poles (thin sheet or formation),
n = 2 is a point pole (narrow vertical pipe),
n = 2 can also be a line of dipoles (sill or channel),
n = 3 is a point dipole (spheres and ellipsoids).

The dimensionality index (I) provides the AI system with some help by using the pipe or sphere models for high dimensionality and the sheet for low dimensionality. The vertical gradient and anomaly amplitudes are derived directly from the pre-processed data. Note also that the vertical gradient is a 2D gradient derived from the grid processing rather than a 1D gradient derived from the line data.

Peters Length Method
Peters Length (Peters, 1949) is a robust analysis method that produces a depth estimate for almost any anomaly shape. Peters Length is defined as the distance between two half-slope points where the slope is defined by the maximum gradient of the anomaly. The half-slope points are easily computed from the horizontal gradient. A correction factor is used to convert the Peters Length distance to depth. The factor is dependent on the geological shape in a similar way to the Euler 2D method. The AI system has calibrated the factors by using a range of standard models.

Werner Deconvolution Method
The Werner Deconvolution method was published by Werner (1953) and is used for determining the depth to a magnetic sheet or edge. We have simplified the method to include one sheet and a linear regional because our method is designed to interpret individual anomalies through user selection. The equation can be simplified to;

$$B_m = \frac{a_1 z_0 + b_1\,(x - x_0\,)}{(x - x_0\,) + z_0} + (c_1 + c_2\, x) \qquad (12)$$

Where;
B_m is the total field as a function of *x*,
x is the location of the data point,
x_0 is the location of the centre of the sheet or edge,
z_0 is the depth to the sheet or edge,
a_1, b_1 are body geometry constants,
c_1, c_2 are first order regional coefficients.

We know the location of the centre of magnetisation (x_0) from the NSS peak position. This equation is computed for multiple x locations and the matrix of equations is solved for the source parameters using singular value decomposition.

Tilt Depth Method

Salem et al. (2007) defined the tilt angle of the magnetic field as;

$$Tilt = tan^{-1}\left((\delta B_m/\delta z) \;/\; (\partial B_m/\partial h)\right) \qquad (13)$$

where;

$$\partial B_m/\partial h = ((\partial B_m/\partial x)^2 + (\partial B_m/\partial y)^2)^{1/2}.$$

The depth is derived directly from the tilt angle using the formula,

$$Tilt = tan^{-1}(h/z) \qquad (14)$$

where h is half the distance between the +45 degree tilt and -45 degree tilt angles on either side of the wide body edge. The method does not require the location of the contact, but it can be derived from the NSS peak or zero Tilt location.

Euler 3D Method

We use the tensor method for calculation of the Euler 3D solution (Schmidt et al, 2004) which uses both the tensor and magnetic field components to solve for the 3D structural index (n) and depth. The basic formulation is shown in their equation (23) as follows,

$$\begin{bmatrix} \frac{\partial B_x}{\partial x} & \frac{\partial B_x}{\partial y} & \frac{\partial B_x}{\partial z} \\ \frac{\partial B_y}{\partial x} & \frac{\partial B_y}{\partial y} & \frac{\partial B_y}{\partial z} \\ \frac{\partial B_z}{\partial x} & \frac{\partial B_z}{\partial y} & \frac{\partial B_z}{\partial z} \end{bmatrix} \begin{bmatrix} x - x_0 \\ y - y_0 \\ z - z_0 \end{bmatrix} = -n \begin{bmatrix} B_x \\ B_y \\ B_z \end{bmatrix} \qquad (15)$$

where the tensor appears on the left-hand side and the field components on the right. The map location for the centre of magnetisation (x_0 , y_0) is known from the peak location of the normalised source strength (NSS) and the equation is solved for z_0 at five critical points along the profile.

The field components are calculated by Fourier transformation of the total magnetic intensity grid and assume that the local regional has been removed. This method is very sensitive to an incorrect regional estimation which feeds through to errors in the three field components. The structural index n is initiated from the tensor analysis but the interpreter can override the choice made by the AI system.

AI SYSTEM

By combining the precision of the flight line data with the 2D information inherent in the gridded magnetic data we provide the essential inputs to the AI process. The tensor analysis provides the primary input to the AI system and the auxiliary channels such as the magnetic field components, gradients, tilt and reduction to pole (RTP) provide the additional input required by the various geophysical methods (Euler, Werner etc.). From these inputs, the AI system can compute depth, azimuth, magnetic susceptibility, depth quality and remanence indicators (Figure 2(b)).

The AI system is focused on using the primary data inputs from the tensor analysis to present a model interpretation based on what it sees as the most probable geological style (dyke, pipe etc.). This model is matched with each of the depth calculation methods unless it is incompatible. For example, the Tilt method is not appropriate for any model other than an edge. By using the various depth analysis methods, the following model styles can be used to compute depths;

- Sheet - thin, medium, thick,
- Pipe – thin, medium thick,
- Sphere/ellipsoid,
- Channel,
- Edge.

An interpreter starts by selecting the anomalous section of data to be interpreted (Figure 2(a)) and the AI system presents a summary of the interpretation results along with its choice of model and method (Figure 2(b)).

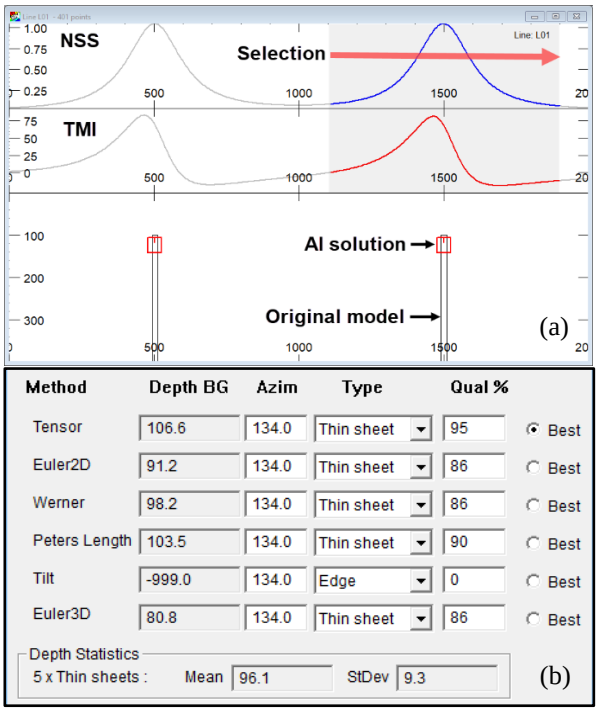


Figure 2. An anomaly is selected in a flight line cross-section (a) and the results presented in a summary table (b). The interpreter can override the Azimuth, model type and method where appropriate. This training set was applied to model data where the sheet model was at a depth of 100m.

In the future, we hope to be able to train the AI system to correctly identify ellipsoids and channels. This will require improvements to the 3D Euler method which returns an optimum structural index, but requires further work on separation of the 2D regional magnetic field.

Most of the depth information in a magnetic anomaly is associated with the steep gradient sections on either side of the anomaly between the major changes in curvature near the anomaly peak and trough. The AI algorithm gathers information that is closely associated with this segment of the anomaly. Instead of using the original total field intensity anomaly, we use the NSS trace because it enhances the depth sensitive section of the anomaly. The NSS trace also has the benefit of being semi-independent of the IGRF inclination with depths from both sides of the anomaly producing similar results.

MODEL TESTS

The AI system is trained on a suite of forward calculated models and tuning parameters are used to create a suite of tables and rules. We see a future role for neural net techniques to improve some of the inputs to the expert system.

Figure 3 shows the results of a synthetic data set test used during the training process with the depth results plotted in cross-sections. The symbols are plotted over the original models for validation. Each model is set to a depth of 100 metres and in the case of the ellipsoid, this is the centre. The three different sheets thickness models have depth errors ranging from 6 to 14%, while the pipe models vary from 0 to 36%. The largest error (136m depth) is associated with the thick pipe and this is caused by applying the thin pipe parameters across all three classes.

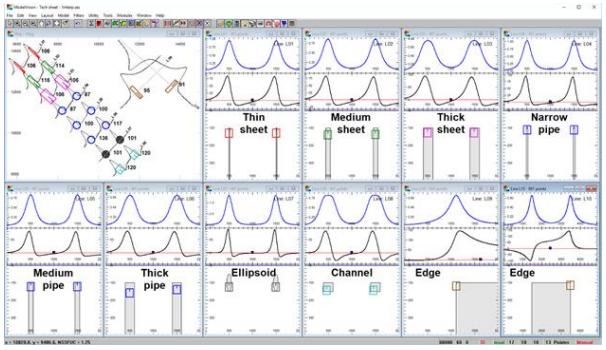


Figure 3. A training dataset with all model types and two bodies per line with all models at a depth of 100m below the sensor. The original models are shown in a series of sections with the AI interpreted results plotted on the models. Different shaped symbols are used in the map view to represent the different model types with depth annotations alongside.

Additional training of the AI system is required to achieve improved results. The error for the ellipsoid model is just 1%. The channel depth appears to be overestimated, but it is only possible to detect the channel centre at 125 metres which puts the depth error at 1%.

Limitations

This AI approach pushes non-inversion methods to another level, especially with the controls over the choice of model style. However, there are limitations that must be considered.

The depth-to-width ratio is the depth to the top of the target divided by the width of the target. At one limit it is a thin sheet like a narrow dyke and at the other extreme it is the edge of a wide body. We use the AI system to partition the range into the categories, thin, medium, thick and edge which improves the precision of the depth estimation.

Interference between adjacent magnetic rock units distorts the curvature and gradients between them and invariably underestimates the depth to the top. The AI system can recognise this interference in the normalised source strength profile and downgrades the quality of the depth estimation result according to the proportion of overlap. The regional magnetic field has a minor impact on the tensor, Peters Length and Werner Deconvolution methods, but it can be severe for the Euler 2D, Euler 3D and Tilt methods.

CASE HISTORY

We have selected a dataset from the Mt Isa Province that has been flown at a line spacing of 200 metres (Figure 4). A subset of the survey data was selected on the edge of the Mt Isa Province where the unconformity surface dips to the east below the Carpentaria Basin sediments.

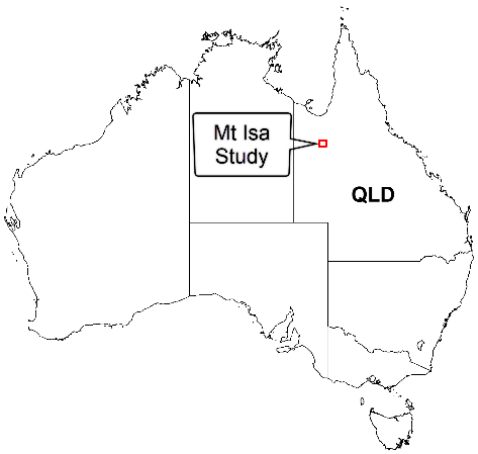


Figure 4. Locality map of the depth interpretation study over the eastern edge of the Mt Isa Province.

A subset of representative flight lines was chosen for the depth study and the results are presented in Figure 5. The left-hand map shows symbols superimposed on a monochrome TMI image where the symbols are oriented according to the strike direction. The black, 50 metre depth contours show the shape of the basin sediments. The contours were generated by gridding the interpreted

depth solutions. The right-hand map shows the annotated depths superimposed on a colour image of the total magnetic intensity.

Figure 5 also shows a selection of cross-section profiles with depth solution symbols in the lower track. The middle track shows the TMI (black) and upper track the normalised source strength (NSS) in blue. The depth sections show the basement shallowing to the west where it eventually outcrops. Individual symbols are colour coded by the depth calculation method, but it is also useful to use other parameters such as depth quality, susceptibility or model type.

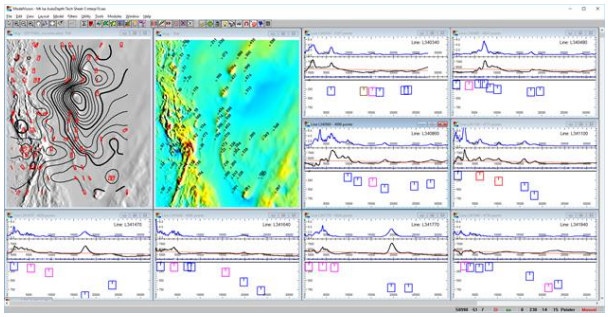


Figure 5. The left-hand map shows azimuth-oriented symbols where depth estimates were obtained and superimposed on a monochrome image of the TMI and contours of basement depths derived from the depth solutions. The right-hand map shows the depth values superimposed on a colour image of the TMI. A selection of cross-sections show depth solutions with graphs of the TMI (black) and NSS (blue).

CONCLUSIONS

The integration of original, high resolution, 1D flight line data with the additional 2D spatial information derived from the total magnetic intensity grid provides a new method for the recovery of depth and magnetic property information. FFT processing of the TMI grid produces the magnetic tensor, magnetic components, TMI derivatives and RTP grids. The resampling of grids onto the 1D flight lines adds the essential 2D spatial information that provides the foundation for the AI system approach to interpreting the data.

The precision of depth estimation is strongly dependent on the correct choice of an appropriate geological model. The AI system is used to assist the interpreter by differentiating between pipes, plutons and elongate geological styles. The AI system uses parameters derived from the magnetic tensor to determine the strike direction, horizontal centre of magnetisation, a depth value, width and magnetic reversal indicator based on the interpreter's final choice of model style. With this starting point, other depth methods are evaluated to provide the interpreter with a spread of results and the opportunity to select the most robust solution.

The automated building of a model based on the AI system provides an excellent seed model for inversion. While the AI system results may not be as precise as those provided by full inversion, they do provide a rapid and practical method for evaluating the depth of cover over large survey areas. Inversion can be used on occasional solutions to QC the interpreter's results.

ACKNOWLEDGMENTS

The work on this project was partially supported by Rio Tinto and the authors would like to thank Theo Aravanis who first suggested the use of the multiple classical depth methods to help assess the variance in depth estimation methods. The AI system was developed and tested in ModelVision (Pratt et al., 2018) and the examples presented here were produced by ModelVision.

REFERENCES

Beike, M., Clark, D.A., Austin, J.R. & Foss, C.A. 2012, Estimating source location using normalized magnetic source strength calculated from magnetic gradient tensor data: Geophysics, 77, (6), J23-J37.

Clark, D.A., 2012, New methods for interpretation of magnetic vector and gradient tensor data I: eigenvector analysis and the normalised source strength: Exploration Geophysics, 43, 267-282.

Clark, D.A. 2014, Methods for determining remanent and total magnetisations of magnetic sources – a review. Exploration Geophysics, 45, 271-304.

Nelson, J.B. 1988, Comparison of gradient analysis techniques for linear two-dimensional magnetic sources. Geophysics 53, (8), p. 1088–1095.

Pedersen, L.B. & Rasmussen, T.M., 1990, The gradient tensor of potential field anomalies: Geophysics, 55 (12), 1558-1566.

Peters, L.J. 1949, The direct approach to magnetic interpretation and its practical application. Geophysics, 14(3), 290-320.

Pratt, D.A., McKenzie, K.B., White, A.S., Foss, C.A., Shamin, A. and Shi, Z., 2001 A user guided expert system approach to 3D interpretation of magnetic anomalies. Extended Abstracts, ASEG 15th Geophysical Conference and Exhibition, Brisbane.

Pratt, D.A., Parfrey, K., White, A.S. & McKenzie, K.B. 2018, ModelVision v16.0 User Guide, pub. Tensor Research, 599p.

Salem, A., Williams, S., Fairhead, J.D., Ravat, D. and Smith, R. 2007, Tilt-depth method: A simple depth estimation method using first-order magnetic derivatives. Leading Edge, 26(12), p. 1502-1505.

Thompson, D.T., 1982, EULDPH: A new technique for making computer-assisted depth estimates from magnetic data. Geophysics, 47(1), p. 31-37.

Werner, S. 1953, Interpretation of magnetic anomalies at sheet-like bodies. In Sveriges Geologiska Undersok Series C.C. Arsbok 43, N:06.

Wilson, H., 1985, Analysis of the magnetic gradient tensor. Defence Research Establishment Pacific, Canada, Technical Memorandum, 85–13, 47.